Finite Volumes for Complex Applications

Problems and Perspectives

editors

Fayssal Benkhaldoun
Roland Vilsmeier

HERMES

Editions Hermès
14, rue Lantiez
75017 Paris

ISBN 2-86601-556-8

Catalogage Electre-Bibliographie

Finite Volumes for Complex Applications : problems and perspectives / dir. Fayssal Benkhaldoun, Roland Vilsmeier. - Paris : Hermès, 1996.
ISBN 2-86601-556-8
RAMEAU : éléments finis, méthode des
analyse numérique
DEWEY : 515 : Analyse mathématique

A Reliable and Accurate Technique For Modelling Complex Open Channel Flows

P A Sleigh[†], *P H Gaskell*[†], *M Berzins*[‡]
† *Department of Mechanical Engineering,*
‡ *Department of Computer Studies,*
University of Leeds,
Leeds, LS6 9JT, UK.

ABSTRACT *It is shown that the solution of challenging, time-dependent hydraulic flow problems can be achieved via the judicious application of a numerical algorithm comprised of state-of-the-art components. The governing equations are discretized using a finite volume formulation consistent with triangular decomposition of the associated domains. Key features are: convective fluxes determined via the solution of local Riemann problems; second order accurate spatio-temporal discretization; local error estimates. Solutions to two problems, one naturally occurring the other man-made, are presented which demonstrate effectively the width of applicability of the algorithm.*

Key Words: Finite Volume, Unstructured Mesh, Error Estimates

1. Introduction

Rivers, estuaries and many other open channel flows can be modelled adequately in terms of the shallow water equations, which can be written in two-dimensional form as:

$$U_t + E_x + G_y = S(U), \tag{1}$$

with $U = [\phi, \phi u, \phi v]^T$ and

$$E = \begin{bmatrix} \phi u \\ \phi u^2 + \frac{1}{2}\phi^2 \\ \phi uv \end{bmatrix}, G = \begin{bmatrix} \phi v \\ \phi uv \\ \phi v^2 + \frac{1}{2}\phi^2 \end{bmatrix}, S = \begin{bmatrix} 0 \\ g\phi(Sf_x + So_x) \\ g\phi(Sf_y + So_y) \end{bmatrix}. \tag{2}$$

where u, v are the velocities in the x, y directions respectively, $\phi = gh$, h is the depth, g is the acceleration due to gravity; $So_{x/y}$ and $Sf_{x/y}$, are x/y bed and friction slopes. The latter is found using either the Manning or (equivalent) De Chezy formulae.

Accordingly, considerable effort has been expended in recent years on obtaining accurate numerical solution to (1), see for example Toro[TOR 92] and Tan [TAN 92]. However, there has been very little corresponding progress in evolving an approach which integrates such ideas into a practically applicable solution algorithm. Those which do exist are usually centred around a rectangular grid system and embody traditional solution and discretization schemes which may lack the required accuracy and may be limited in range of capability [FAL 92]. A notable exception is the approach adopted by Zhao *et al* [ZHA 96] who integrated the latest shock capturing methods into a complete, albeit first order accurate, river model.

The present work brings together many of the latest numerical and computational techniques with a view to providing a satisfactory answer to the above, and employs the following key components:

- a finite volume formulation, the unstructured computational grid for which is generated automatically by triangular decomposition of the region of interest; any associated digital bathymetry data is similarly interpolated automatically;
- the use of an appropriate Riemann solver to calculate inter-cell convective fluxes together with an associated flux limiter which is monotonicity preserving;
- 2nd order accurate spatial and temporal discretization and efficient solution of the associated algebraic equation set via SPRINT2D;
- the flexibility to specify general boundary conditions, including the capacity to handle wetting and drying characteristics.[SLE 96]

The test problems to be investigated are: i) coastal flow around a Pacific island; ii) flow through a complex recreational water facility.

2. Algorithmic Formulation

A cell centred finite volume method is formulated by integrating equations (1) over a triangular shaped control volume, representing the dependent variables of the system as piecewise constants associated with the centroid. Integrating equations (1) over the ith triangle, say, gives:

$$\int_{A_i} \frac{\partial U}{\partial t} d\Omega - \int_{A_i} S(U) d\Omega = - \int_{A_i} (E(U)_x + G(U)_y)\, d\Omega \qquad (3)$$

where A_i is the area of the triangle and Ω is the integration variable defined on A_i. The integrals on the left are evaluated via a one-point quadrature rule – the quadrature point being the centroid of the triangle, with velocity U_i. Using the divergence theorem, the area integral on the right can be written as a line integral along the boundary:

$$A_i \frac{\partial U_i}{\partial t} = -\oint_{\Gamma_i} F_n(U)dS + A_i S(U) \tag{4}$$

where Γ is the periphery of the triangle and S is the associated integration variable. Using a mid-point quadrature rule to approximate the integral enables the flux at the mid-point of each side of the triangle to be written as:

$$\frac{\partial U_i}{\partial t} = -\frac{1}{A_i}\left(F_n(U)_{ik}.l_{ik} + F_n(U)_{ij}.l_{ij} + F_n(U)_{il}.l_{il}\right) + S(U_i), \tag{5}$$

where ij represents a common edge, of length l_{ij}, of two triangles with associated velocities U_i and U_j, and $F_n(U)_{ij}$ the flux (from the triangle associated with U_i) in the outward normal direction, evaluated at the mid-point of this edge. These are defined similarly for sides ik and il. [BER 95, SLE 96]

The unstructured triangular meshes used to perform the computations were generated using public domain software, GEOMPACK [JOE 91], which was found to produce consistently 'smooth' meshes with an outline of the domain and a triangle 'quality value' only needing to be specified. An added feature is that GEOMPACK also allows the mesh to be distributed as required via a function defining a weight between 0 and 1 at any point in the domain. Hence the mesh density can be conveniently increased in regions having known geometric complexity, interesting flow features or high levels of error.

A feature of equations (1) which is extremely useful is that they are rotationally invariant enabling the use of one-dimensional solution schemes based on a local co-ordinate system, $(\bar{x}, \bar{y})$ say, centred at the mid-point of a cell face. In which case the solution to:

$$\overline{U}_t + \left(E(\overline{U})\right)_{\bar{x}} = 0, \tag{6}$$

where $E(\overline{U}) = [\phi u_n, \phi u_n^2 + \frac{1}{2}\phi^2, \phi u_n u_t]^T$ is transformed back to the global coordinate system giving the flux, $F_n(U)$, at each face in equation (5).

The evaluation of the normal flux, equation (5), is posed as a series of Riemann problems, local to the lines which make up the triangular mesh. Each one is an initial value problem with discontinuous conditions on either side of the line, the approximate solution to which enables the correct flux value, $E(\overline{U})$, in equation (6) to be computed. Tan[TAN 92] and Toro[TOR 92] identify several suitable approximate Riemann solvers. However, following a series of exhaustive one-dimensional tests Roe's solver was found to be the most robust.

Riemann solvers are also convenient in the context of boundary conditions, since for a particular problem these can be applied by replacing one side of the Riemann problem with a relationship describing the conditions at the boundary. It is solved in the same way as those in the interior of the domain to obtain a flux across the boundary.

Second order accurate spatial discretization is achieved by writing, Berzins and

Ware[BER 95]:

$$\left.\begin{array}{rcl} U_L & = & U_i + \Phi(r^l_{ij})\left(U^L_{ij} - U_i\right) \\ U_R & = & U_j + \Phi(r^r_{ij})\left(U^R_{ij} - U_j\right) \end{array}\right\} \quad (7)$$

where U^L_{ij} and U^R_{ij} are the internal and external linear upwind values; r^l_{ij} and r^r_{ij} are the internal and external upwind bias ratios of gradients, defined as:

$$r^l_{ij} = \frac{U^C_{ij} - U_i}{U^L_{ij} - U_i}, \; r^r_{ij} = \frac{U^C_{ij} - U_j}{U^R_{ij} - U_j}, \quad (8)$$

where U^C_{ij} is the linear centred value at the cell interface. Φ is a modified Van Leer flux limiter and the values of U^L_{ij}, U^R_{ij} and U^C_{ij} are determined from a series of one-dimensional linear interpolations from a six-triangle stencil.[BER 95]

Time integration was carried out within the SPRINT2D environment using a explicit, Theta method in which the solution at time $t_{n+1} = t_n + \kappa$, where κ is the time step, is written as:

$$\underline{V}(t_{n+1}) = \underline{V}(t_n) + (1+\theta)\kappa\dot{\underline{V}}(t_n) + \theta\kappa\underline{F}_N(t_{n+1}, \underline{V}(t_{n+1})) \quad (9)$$

where $\underline{V}(t_n)$ and $\dot{\underline{V}}(t_n)$ is the numerical solution and its time derivative at the previous time, t_n, respectively. The value of θ is constrained to lie in the range $0.5 \leq \theta < 1.0$. However, its value was pre-set explicitly at 0.55. κ is chosen to satisfy a local error control which may reflect the spatial error present. The system of equations is solved by functional iteration and it can be shown how an associated CFL type stability condition is satisfied automatically if the functional iteration converges sufficiently fast, [BER 95, SLE 96].

For each of the triangles which comprise the solution domain a local spatial error estimate is made, based on the difference between solutions found with both a low and high order interpolation scheme, for each equation. A scaled error is then computed for each of them, using prescribed absolute and relative errors, as a means of providing a measurement for use as suitable refinement indicator. This approach is very flexible, and provides the basis from which to implement automatic grid refinement/coarsening. An alternative approach, used here, is to make the necessary mesh adjustments affected via the redistribution functions available within GEOMPACK.

3. Problem Specification and Results

First the flow in the shallow coastal waters around Rattray Island, which lies off the north-east coast of Australia, is examined. The island is approximately 1.5km long and 0.3km wide and inclined at 60° to the dominant tidal current; the mean local depth is approximately 25m. Observers of the flow past this island have noted that it is predominantly unidirectional with in a large eddy to the lee-ward side. Previous two-dimensional theoretical investigations [FAL 92] of the flow have shown good agreement with available field data, indicating that equations (1) constitute a suitable model. In line with previous numerical studies the flow domain and attendant boundary conditions are shown in Figure 1 with the boundary data supplied from field measurements. Slope friction is incorporated via the Manning formula with $n = 0.025$.

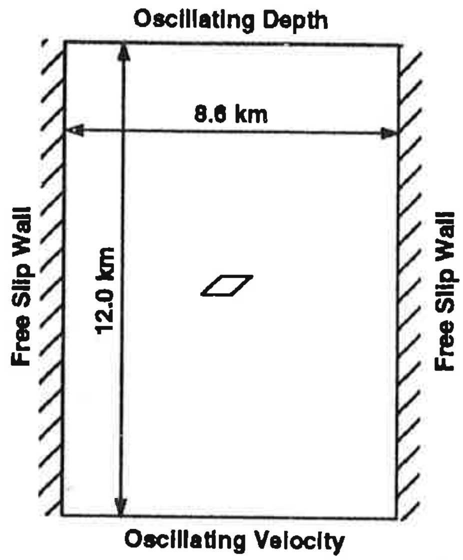

Figure 1: Domain Dimensions and Boundary Conditions.

Sample results after 24003 seconds have lapsed are shown if Figure 2 – to the left the mesh for the entire domain, to the right, close ups of the velocity field on the leeward side of the island. Looking from top to bottom it can be seen that with 986 cell mesh only, two rather ill defined vortices exist downstream of the island. Although it is obvious visibly that this area requires a finer mesh, the same is indicated by the solution since the errors in this region were found to be higher. The middle figures show the result of increasing the total mesh density, in a regular sense, to 3983 cells. Resolution of the two vortices is now much better but there are far too many cells in regions of the flow where very little is happening for the required level of accuracy. The bottom figures demonstrates the effect of implementing the redistribution features within GEOMPACK. Here a 2033 cell mesh is used to concentrate the majority of cells in the high error region. The two vortices remain as equally well defined as for the middle mesh yet roughly half the number of cells have been used.

The second problem considered is that of flow in a prototype canoe slalom, see Figure 3 – it is approximately $200m$ long having a flow rate typical of such large scale facilities and equal to $10m^3/s$. Note how this domain contains islands which present no additional difficulty for the mesh generation procedure.

The boundary conditions are such that there is no flow across the containing walls; the upstream flow rate is as specified above and at the downstream end a depth of $0.8m$ is prescribed. Figure 3 shows the course tessellated with 1335 triangular cells. This serves to illustrate both the complexity of the flow domain itself and the nature of the triangular decomposition. Shown also are: (a) the steady-state velocity vectors in the second pond obtained with the the above mesh; (b) the mesh covering the same pond

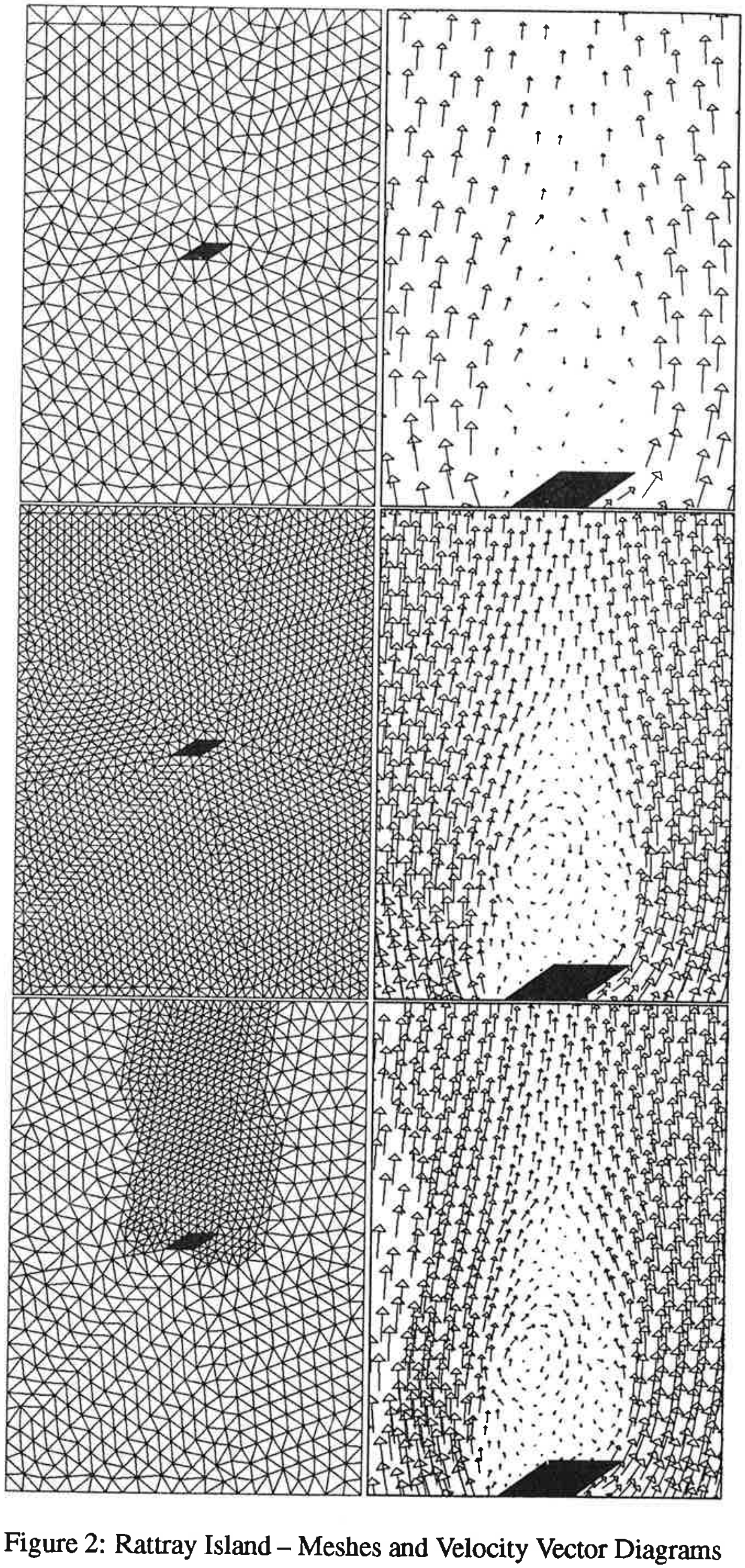

Figure 2: Rattray Island – Meshes and Velocity Vector Diagrams

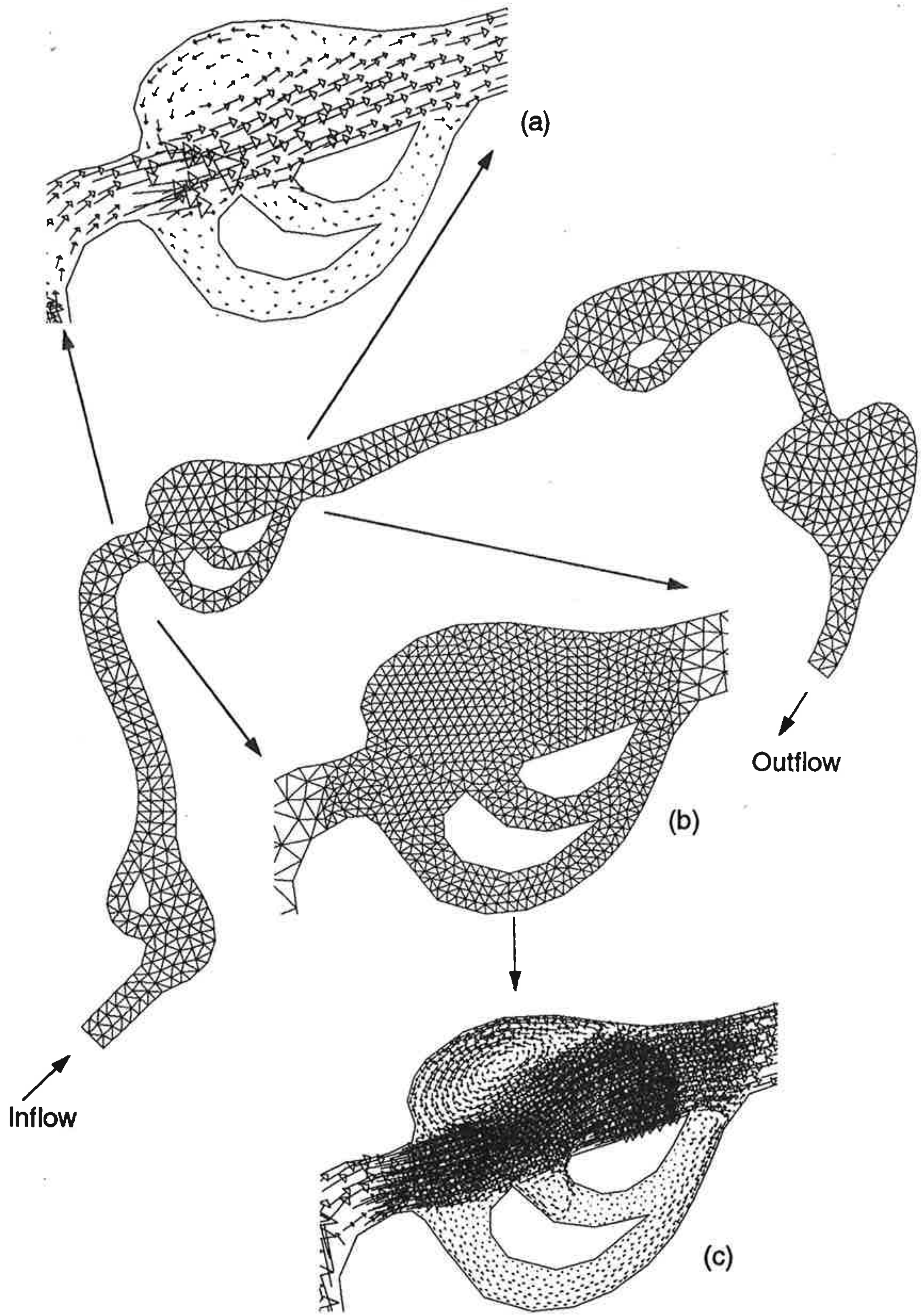

Figure 3: Canoe Course – Meshes and Velocity Vector Diagrams

obtained using 2323 tria gles in total but weighted towards this region; (c) the corresponding velocity vectors obtained with the weighted mesh.

The two sets of velocity vectors are in accord and reveal an interesting flow pattern, while the bulk of fluid follows a path straight through the pond, in doing so it generates a reverse flow along the entire length of ponds lowest branch, a large eddy in the upper section and perhaps most interesting of all a small eddy in the neck of the second branch. The resolution of detailed features such as these now offer the designers of such recreational facilities a new tool in their search for the best possible design.

Acknowledgements

The authors wish to thank the EPSRC for funding P.A.Sleigh through Grant GR/J09901, Shell Research Ltd apropos the SPRINT2D software project together with R. Falconer, University of Bradford, and E.Wolanski, Australian Institute of Marine Science, for providing the Rattray Island data.

[ALC 93] Alcrudo F and Garcia-Navarro P. A high-resolution Godunov-type scheme in finite volumes for the 2d shallow-water equations. *International Journal For Numerical Methods In Fluids*, Vol.16(No.6):pp.489–505, 1993.

[BER 95] Berzins M and Ware JL. Positive cell-centred finite volume discretisation methods for hyperbolic equations on irregular meshes. *Applied Numerical Mathematics*, Vol.16, pp.417–438, 1995.

[FAL 92] Falconer RA and Li Gy. Modeling tidal flows in an islands wake using a 2-equation turbulence model, *Proceedings Of The Institution Of Civil Engineers-Water Maritime And Energy* Vol.96, No.1, pp.43-53, 1992

[JOE 91] Joe B and Simpson RB. Triangular meshes for regions of complicated shape. *International Journal For Numerical Methods in Engineering*, Vol.23:pp.987–997, 1991.

[SLE 96] Sleigh P A, Berzins M, Gaskell P H and Wright N G An Unstructured Finite volume method for predictiong flow in rivers and estuaries Submitted to *Journal Of Hydraulic Research*, 1996.

[TAN 92] Tan WY. *Shallow Water Hydrodynamics*. Elsevier Oceanography Series. Elsevier, 1992.

[TOR 92] Toro EF. Riemann problems and the WAF method for solving the 2-dimensional shallow-water equations. *Philosophical Transactions Of The Royal Society Of London Series A-Physical Sciences And Engineering*, Vol.338(No.1649):pp.43–68, 1992.

[ZHA 96] Zhao DH, Shen HW, Tabios GQ, Lai JS, and Tan WY. Finite-volume 2-dimensional unsteady-flow model for river basins. *Journal Of Hydraulic Engineering-ASCE*, Vol.120(No.7):pp.863–883, 1994.